

Dual mTORC1/mTORC2 inhibition diminishes Akt activation and induces Puma-dependent apoptosis in lymphoid malignancies

*Mamta Gupta,¹ *Andrea E. Wahner Hendrickson,¹ Seong Seok Yun,¹ Jing Jing Han,¹ Paula A. Schneider,¹ Brian D. Koh,¹ Mary J. Stenson,¹ Linda E. Wellik,¹ Jennifer C. Shing,¹ Kevin L. Peterson,¹ Karen S. Flatten,¹ Allan D. Hess,¹ B. Douglas Smith,^{1,2} Judith E. Karp,^{1,2} Sharon Barr,^{1,3} †Thomas E. Witzig,¹ and †Scott H. Kaufmann¹

¹Departments of Medicine, Oncology and Pharmacology, Mayo Clinic, Rochester, MN; ²Sidney Kimmel Cancer Center at Johns Hopkins, Baltimore, MD; and ³OSI Pharmaceuticals, Farmingdale, NY

The mammalian target of rapamycin (mTOR) plays crucial roles in proliferative and antiapoptotic signaling in lymphoid malignancies. Rapamycin analogs, which are allosteric mTOR complex 1 (mTORC1) inhibitors, are active in mantle cell lymphoma and other lymphoid neoplasms, but responses are usually partial and short-lived. In the present study we compared the effects of rapamycin with the dual mTORC1/mTORC2 inhibitor OSI-027 in cell lines and clinical samples representing divers lymphoid malignancies. In

contrast to rapamycin, OSI-027 markedly diminished proliferation and induced apoptosis in a variety of lymphoid cell lines and clinical samples, including specimens of B-cell acute lymphocytic leukemia (ALL), mantle cell lymphoma, marginal zone lymphoma and Sezary syndrome. Additional analysis demonstrated that OSI-027–induced apoptosis depended on transcriptional activation of the PUMA and BIM genes. Overexpression of Bcl-2, which neutralizes Puma and Bim, or loss of procaspase 9 diminished

OSI-027–induced apoptosis in vitro. Moreover, OSI-027 inhibited phosphorylation of mTORC1 and mTORC2 substrates, up-regulated Puma, and induced regressions in Jeko xenografts. Collectively, these results not only identify a pathway that is critical for the cytotoxicity of dual mTORC1/mTORC2 inhibitors, but also suggest that simultaneously targeting mTORC1 and mTORC2 might be an effective anti-lymphoma strategy in vivo. (*Blood*. 2012;119(2):476-487)

Introduction

Despite being considered among the most treatable malignancies, lymphomas and lymphocytic leukemias continue to account for more than 27 000 deaths annually in the US¹ These statistics highlight the continued need for improved therapy.

Over the past 6 years, rapamycin and its derivatives temsirolimus and everolimus (collectively called rapalogs) have shown promising activity in a wide range of lymphoma subtypes.² These agents are allosteric inhibitors of the mammalian target of rapamycin (mTOR), a highly conserved serine/threonine kinase that integrates signaling from the phosphoinositide-3-kinase (PI3K)/Akt and AMP kinase pathways as well as others (reviewed in Bjornsti and Houghton,³ Dowling et al,⁴ and Sengupta et al⁵). Through its involvement in 2 distinct complexes, mTOR complex 1 (mTORC1) and mTORC2, mTOR modulates several processes, including mRNA translation, cell cycle progression, survival and motility.^{4,6} In particular, the raptor-containing mTORC1 phosphorylates p70 S6 kinase and eukaryotic initiation factor 4E binding protein 1 (4E-BP1), thereby regulating translation of certain messages that are critical for progression from G₁ into S phase (cyclin D1, c-myc) and, in some cells, survival (Mcl-1 and Bcl-x_L).^{4,7} In addition, the rictor-containing mTORC2 phosphorylates Akt on Ser⁴⁷³, affecting Akt-mediated survival signaling, and AGC family kinases,^{4,6} thereby modulating cell motility.

The effects of rapalogs on signaling are complex. After rapamycin initially binds to the cytosolic protein FKBP12, the

resulting complex interacts with the FK-rapamycin binding domain of mTOR and selectively disrupts mTORC1 assembly.^{8,9} As a consequence, phosphorylation of mTORC1 substrates decreases, with some substrates being affected more than others.^{10,11} Although mTORC1 inhibition would be expected to diminish cell survival, the extent of killing can be reduced by additional changes that occur, including Akt activation because of phosphorylation on Ser⁴⁷³, which reflects inhibition of negative feedback loops in some cell types.^{5,12,13} Alternatively, prolonged rapalog treatment decreases mTORC2-induced Akt activation in other cells.¹⁴

Because responses of lymphomas to rapalogs in the clinic, while promising, are often partial and transient,² there has been substantial interest in enhancing the antineoplastic actions of these agents.^{4,8,15} Toward this end, nonrapamycin-based, active site-directed mTOR inhibitors that target both mTORC1 and mTORC2 have been developed. One such agent, WYE-132, is not only more effective than rapamycin at inhibiting protein synthesis, cancer cell growth and survival in vitro, but also highly efficacious in multiple solid tumor xenograft models.¹⁶ AZD8055, another dual mTORC1/mTORC2 inhibitor, likewise inhibits protein synthesis potently and suppresses a wide range of solid tumor xenografts.¹⁷ A third dual inhibitor, PP242, has potent cytotoxic activity in Bcr/abl-transformed leukemia cells in vitro and in xenograft models.¹⁸ Despite the activity of rapalogs in lymphoma, the potential activity of this class of agents against lymphoma has not been reported; and

Submitted April 5, 2011; accepted November 2, 2011. Prepublished online as *Blood* First Edition paper, November 11, 2011; DOI 10.1182/blood-2011-04-346601.

*M.G. and A.E.W.H. contributed equally to this article as co-first authors.

†T.E.W. and S.H.K. contributed equally to this article as co-senior authors.

The online version of this article contains a data supplement.

The publication costs of this article were defrayed in part by page charge payment. Therefore, and solely to indicate this fact, this article is hereby marked "advertisement" in accordance with 18 USC section 1734.

© 2012 by The American Society of Hematology

the mechanism of cytotoxicity in dual mTORC1/mTORC2 inhibition in malignant lymphoid cells has not been previously investigated.

OSI-027 is a recently described, potent and selective active site-directed mTOR inhibitor that has been shown to provide greater inhibition of growth than rapamycin in solid tumor models in vitro and in vivo.^{19,20} Earlier studies established its ability to not only inhibit the phosphorylation of mTORC1 and mTORC2 substrates, but also induce apoptosis and autophagy in chronic myelogenous leukemia cells.²¹ The present studies were designed to: (1) assess the antiproliferative and cytotoxic effects of OSI-027 in lymphoma and acute lymphocytic leukemia (ALL) cell lines and clinical samples in vitro; (2) determine its mechanism of cytotoxicity in these cells; and (3) evaluate its activity in a xenograft model.

Methods

Reagents

OSI-027 was synthesized as previously described¹⁹ or purchased from ChemieTek. Reagents were purchased from the following suppliers: annexin V conjugated to FITC or allophycocyanin (APC) from BD Biosciences; phenazine methosulfate, 3-methyladenine, polyethylene glycol 400, Tween-80 and rapamycin for tissue culture from Sigma-Aldrich; the broad spectrum caspase inhibitor Q-VD-OPh²² from SM Biochemicals; NVP-BEZ235 from ChemieTek; rapamycin for animal studies from LC Laboratories; and 3-(4,5-dimethylthiazol-2-yl)-5-(3-carboxymethoxyphenyl)-2-(4-sulfophenyl)-2H-tetrazolium (MTS) from Promega. Antibodies were obtained from the following suppliers: PP1, Bax and β -actin from Santa Cruz Biotechnologies; Puma from ProSci; Noxa from Enzo Life Sciences; and Foxo3a or phospho-Thr³²-Foxo3a from Millipore. Antibodies to all other proteins, including phosphorylated epitopes, were from Cell Signaling Technology.

Samples of lymphoid malignancies

Samples from lymphoma patients were obtained through the University of Iowa/Mayo Lymphoma SPOR Biospecimens Core as surgical waste specimens. Mononuclear cells were isolated from lymph node biopsies by mechanical disruption over a wire mesh screen followed by Ficoll-Hypaque centrifugation. ALL samples were isolated from pretreatment bone marrow aspirates of newly diagnosed patients. All patients signed informed consent in accordance with the Declaration of Helsinki to provide excess tissue for research on Institutional Review Board–approved protocols.

Immunohistochemistry

Slides from formalin-fixed paraffin-embedded tissue blocks were deparaffinized and endogenous peroxidase activity was inhibited by incubation in 1:1 3% H₂O₂:methanol. Samples were then stained using a DAKO autostainer, rinsed, counterstained with hematoxylin and mounted with aqueous mounting media. All images were captured with SPOT RT camera and SPOT Version 4.1 software (Diagnostic Instruments).

Tissue culture

Jeko-1, Mino, DoHH2, and RL cells were obtained from American Type Culture Collection. SeAx cells were a kind gift from S. Ansell (Mayo Clinic). All other cell lines were obtained as previously described.^{23,24} Cell lines were propagated at densities of $< 1 \times 10^6$ cells/mL in RPMI 1640 medium containing 10% heat-inactivated FBS, 100 units/mL penicillin G, 100 μ g/mL streptomycin, and 2mM glutamine (medium A) except for SeAx, JB-6, I9.2, I2.1, and JMR cells, which received medium A supplemented to 15% FBS.

Proliferation assay

Cells were cultured for 48 hours at 37°C in 96-well plates at a density of 5×10^4 cells/well in the presence of OSI-027. Before harvesting, cells were

pulsed with 1 μ Ci [³H]-thymidine (³H-TdR, Amersham) for the last 18 hours. Samples were harvested onto glass fiber filters using a multi-well harvester and washed with H₂O before scintillation counting.

MTS assay

Aliquots containing $\sim 2 \times 10^4$ cells in 120 μ L medium A were incubated at 37°C with varying concentrations of OSI-027 for 5 days. After reaction with MTS and phenazine methosulfate as instructed by the supplier, plates were incubated for 2-6 hours to obtain an absorbance of 0.5-1.0 at 490 nm in control samples.

Assessment of cell killing

After cells were treated with rapamycin or OSI-027 as indicated, DNA fragmentation,²³ annexin V binding^{25,26} and apoptotic nuclear morphologic changes²³ were assayed as described. To determine whether autophagy was induced, cells were transfected²⁷ with plasmid encoding microtubule associated protein 1 light chain 3 (LC3) fused to enhanced green fluorescent protein (LC3-EGFP, Addgene), allowed to express the transgene for 24 hours, and treated for 48 hours with diluent, 10 μ M OSI-027 or 10nM rapamycin. After cytocentrifugation, cells were fixed in 2% (wt/vol) paraformaldehyde in Dulbecco calcium- and magnesium-free phosphate-buffered saline (PBS), permeabilized with 0.2% (vol/vol) Triton X-100 in PBS, stained with 1 μ g/mL Hoechst 33258 in PBS, examined on a Zeiss LSM710 confocal microscope using a 100 \times /1.4 NA objective and scored for punctate cytoplasmic fluorescence, a marker of autophagosome formation.

Immunoblotting

Cells (5×10^6) were incubated with various concentrations of OSI-027 or rapamycin at 37°C in the absence or presence of 5 μ M QVD-OPh as indicated. Cells were washed with cold PBS and lysed with RIPA lysis buffer supplemented with phosphatase and protease inhibitors cocktail (Roche Diagnostics) or as previously described.²⁸ After clarification of the lysates by centrifugation, proteins were resolved by SDS-PAGE and probed using standard techniques.^{26,29}

RT-PCR

After total RNA was isolated from control or OSI-027–treated cells, cDNA was synthesized using a Superscript III First-strand Synthesis kit (Invitrogen) following the supplier's instructions. PCR reactions (50 μ L) were performed using 3 μ g cDNA product and Promega Master Mix PCR reagents according to the supplier's instructions. The following primers were used: Bim forward, 5'-ATGGCAAAGCAACCTTCTGATG-3' and Bim reverse, 5'-TCAATGCATTCTCCACACCAGG-3'; Puma α forward, 5'-CATCCCGGATCCAATGGCCCCGCGCAC-3'; Puma α reverse 5'-CTAATTGGGCTCCATCTCGGGGGCTC-3'; and glyceraldehyde-3 phosphate dehydrogenase (GAPDH) forward, 5'-GGCAAATCCATGGCAC-CGTCAGG-3' and GAPDH reverse, 5'-GGGAGGCATTGCTGATGATCTGAGG-3'. Amplification involved a 3-step program: 95°C for 60 seconds; 35 cycles of 95°C for 30 seconds, 55°C for 30 seconds, 72°C for 60 seconds; and 72°C for 7 minutes. Following amplification, products were electrophoresed on a 2% (wt/vol) agarose gel containing 0.5 μ g/mL ethidium bromide in 1 \times TAE buffer (30.7mM Tris, 20mM sodium acetate and 1mM EDTA), visualized on a UV transilluminator, excised and sequenced using automated dye terminator technology. Alternatively, quantitative RT-PCR (qRT-PCR) was performed in triplicate using 100 ng RNA and TaqMan One-Step RT-PCR Master Mix (Applied Biosystems) per the supplier's instructions. Using Bim (Hs00197982_m1) and Puma (Hs00248075_m1) probe sets, PCR was performed on a ABI Prism 7900HT Real-Time System using a program consisting of 48°C for 30 minutes, 95°C for 10 minutes, then 40 cycles of 95°C for 15 seconds and 60°C for 1 minute. Data analysis was performed using the following equations: $\Delta C_t = C_t(\text{sample}) - C_t(\text{endogenous control})$; $\Delta\Delta C_t = \Delta C_t(\text{sample}) - \Delta C_t(\text{untreated})$; and fold change = $2^{-\Delta\Delta C_t}$.

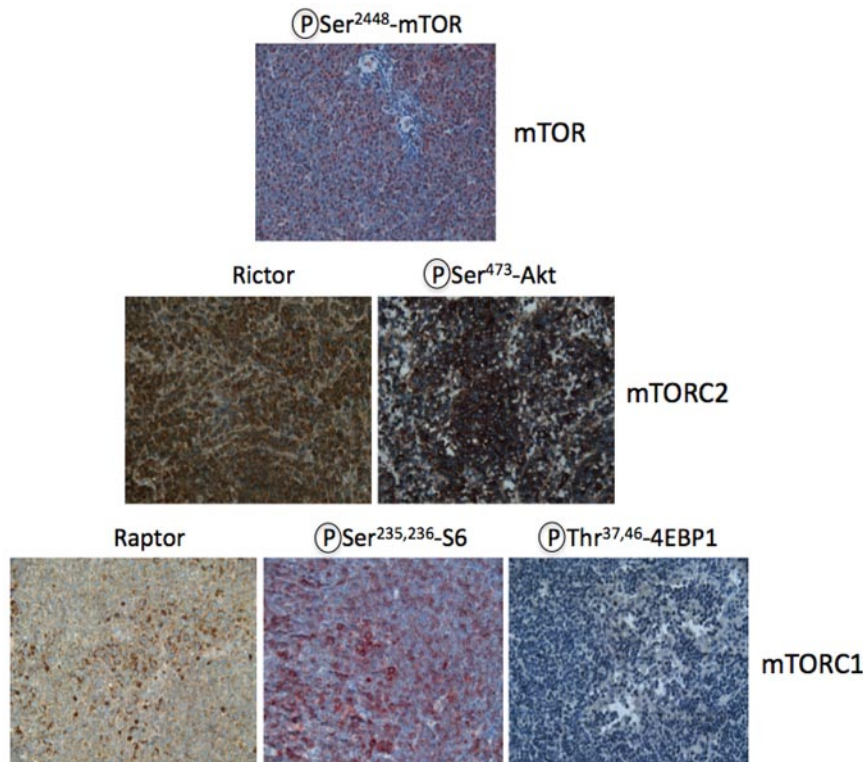


Figure 1. Activation of mTORC1 and mTORC2 signaling in clinical lymphoma samples. MCL samples ($n = 10$) were stained using antibodies to rictor, raptor, and autophosphorylated mTOR as well as phosphorylation site-specific antibodies for targets downstream of mTORC1 (phospho-Thr^{37/46}-4EBP1, phospho-Ser^{235/236}-ribosomal S6 protein) and mTORC2 (phospho-Ser⁴⁷³-Akt). Similar results were observed in all 10 specimens.

Coimmunoprecipitation assay

To lysates prepared as described previously,²⁶ 2–5 μ g of specific antibodies were added and complexes were allowed to form by incubating with rotation overnight at 4°C. A 50% slurry (25 μ L) of protein A-Sepharose was then added and the incubation continued for 2 hours. Immunoprecipitates captured with protein A-Sepharose were washed 3 times with RIPA buffer and analyzed by immunoblotting as described in “Immunoblotting.”

siRNA transfection

Short oligonucleotides targeting Bax (nucleotides 271–289, GenBank accession number NM_138761), Bak (nucleotides 913–931, NM_001188), Bim (nucleotides 325–343, NM_138621), and Puma (nucleotides 784–802, NM_014417) were from Ambion. Transfections were performed as previously described.²⁷

Luciferase assays

Plasmids containing the 0.8 kb Bim promoter³⁰ and the full-length Puma promoter including the regulatory elements between exons 1 and 2³¹ in front of firefly luciferase cDNA were kindly provided by G. Wildey and P. Howe (Cleveland Clinic, Cleveland, OH) and T. Look (Dana Farber Cancer Institute, Boston, MA), respectively. To assess the effect of OSI-027, aliquots containing 5×10^6 log phase Jurkat or SeAx cells cultured in antibiotic-free medium were sedimented, resuspended in 400 μ L antibiotic-free medium containing 40 μ g of reporter construct and transfected by electroporation using a T830 square wave electroporator (BTX) delivering a 240-V pulse for 10 milliseconds. After a 15-minute incubation at 21°C, aliquots containing $\sim 1.3 \times 10^6$ cells were diluted in their tissue culture media, allowed to recover overnight, and treated for 48 hours with diluent (0.1% dimethyl sulfoxide) or the indicated OSI-027 concentration and 5 μ M Q-VD-OPh to prevent apoptosis. At the completion of the drug treatment, cells were sedimented at 200g for 10 minutes, washed twice in PBS, lysed in passive lysis buffer and assayed sequentially for firefly and Renilla luciferase using a Centro XS³ LB 960 plate luminometer (Berthold Technologies).

Xenograft study

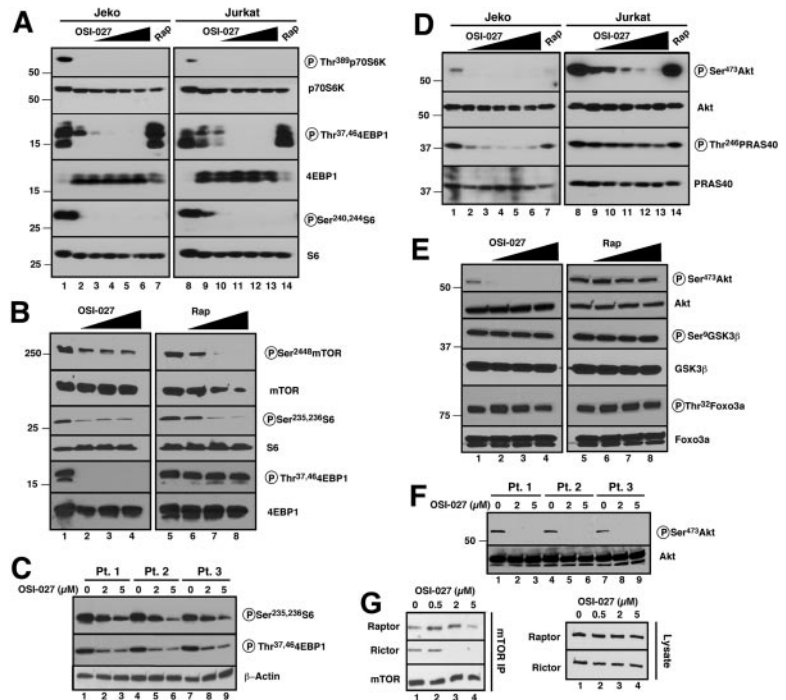
Under a protocol approved by the Mayo Clinic Institutional Animal Care and Use Committee, female athymic nu/nu mice (4–5 weeks, Harlan) were implanted subcutaneously with radiofrequency identification chips along the neck and 100 μ L of a 1:1 slurry containing Matrigel (BD Bioscience) and 5×10^6 washed, log phase Jeko cells in the right flank. Lymphoma volumes were calculated according to the formula $ab^2/2$, where a is the diameter along the longest dimension and b is the orthogonal diameter, respectively. When the lymphomatous masses reached an average of 100 mm³, mice were randomized to receive: OSI-027 58 mg/kg in 20% Trappsol (Cyclodextrin Technologies Development Inc)²⁰ versus vehicle by gavage (experiment 1) or OSI-027 50 mg/kg in Trappsol versus vehicle by gavage versus rapamycin 2 mg/kg³² in sterile water containing 4% (vol/vol) ethanol, 5% (wt/vol) polyethylene glycol 400 (Sigma-Aldrich) and 5% (wt/vol) Tween-80 IP (experiment 2). Animals were treated on days 1–6, 9–14 and 17–22 based on the weight on each treatment day. Five animals per group were followed until lymphomas reached 1.5 cm diameter or day 33. Additional xenografted mice were killed before treatment and on days 3, 5 and 6 of each experimental arm.

Results

mTORC1 and mTORC2 substrates are phosphorylated in clinical lymphoma specimens

Before examining the effect of the dual mTORC1/mTORC2 inhibitor OSI-027 in lymphoid cells, we first examined whether both mTORC1 (rapamycin sensitive) and mTORC2 (rapamycin insensitive) are activated in primary lymphoma specimens. Ten paraffin embedded specimens of MCL, a disease that responds to rapalogs,² were examined by immunohistochemistry. As indicated in Figure 1, staining for raptor (a component of mTORC1) and phosphorylation of the mTORC1 downstream targets ribosomal protein S6 and 4E-BP1 was readily demonstrated, along with

Figure 2. Effects of OSI-027 and rapamycin on phosphorylation of mTORC1 and mTORC2 substrates in malignant human lymphoid lines. (A,D) The MCL line Jeko (left) and T-cell ALL line Jurkat (right) were treated for 8 hours with diluent (lanes 1,8); OSI-127 at 1.25, 2.5, 5, 10 or 20 μ M (lanes 2-6 and 9-13, respectively); or 10nM rapamycin (lanes 7,14). Whole cell lysates²⁸ were then subjected to SDS-PAGE followed by immunoblotting with antibody that recognizes the indicated antigen. (B,E) Jeko cells were treated for 24 hours with diluent (lanes 1,5); OSI-127 at 0.5, 2, or 5 μ M (lanes 2-4); or rapamycin at 1, 10 and 100nM (lanes 6-8). Cell lysates²⁶ were then subjected to SDS-PAGE followed by immunoblotting with antibody that recognizes the indicated antigen. (C,F) Samples from 3 MCL patients were treated for 24 hours with diluent or OSI-127 at 2 and 5 μ M. After SDS-PAGE, cell lysates were probed as indicated. (G) After Jeko cells were treated with the indicated OSI-127 concentration for 24 hours, mTOR immunoprecipitates (top) or cell lysates (bottom) were probed as indicated.



autophosphorylation of mTOR at Ser²⁴⁴⁸. In addition, expression of rictor (a component of mTORC2) and phosphorylation of the mTORC2 substrate Akt Ser⁴⁷³ was also observed. Similar staining was observed in all 10 specimens. These observations, in concert with similar results recently reported in diffuse large cell lymphoma,²⁶ follicular lymphoma,³³ T-cell ALL³⁴ and Philadelphia chromosome-positive ALL,¹⁸ provide a potential rationale for targeting both complexes simultaneously.

OSI-027 and rapamycin have distinct effects on mTORC1 and mTORC2 targets

In view of the preceding results, we compared the effects of therapeutically achievable concentrations of OSI-027 and rapamycin in cell lines derived from a variety of lymphoid malignancies, including B-cell [mantle cell lymphoma (Jeko, Mino), follicular lymphoma (RL)] and T-cell disorders [T-cell ALL (Jurkat) and Sezary syndrome (SeAx)]. Initial experiments focused on the phosphorylation of mTOR substrates in the MCL line Jeko and the T-cell ALL line Jurkat. After 8 hours of treatment, OSI-027 inhibited phosphorylation of all mTORC1 substrates examined, including p70 S6 kinase and its substrate ribosomal protein S6 at Ser²⁴⁰ and Ser²⁴⁴ as well as 4E-BP1 at Thr³⁷ and Thr⁴⁶ (Figure 2A). In contrast, rapamycin inhibited phosphorylation of ribosomal protein S6 but not 4E-BP1 at these sites (Figure 2A lanes 7 and 14), in agreement with earlier reports that some mTORC1 substrates are affected more than others by rapamycin.^{10,11} Similar results were observed at longer time points and with higher rapamycin concentrations (Figure 2B), ruling out the possibility that persistent 4E-BP1 phosphorylation simply reflected sluggish 4E-BP1 dephosphorylation. Consistent with these results, OSI-027 also inhibited phosphorylation of both ribosomal S6 and 4E-BP1 in clinical MCL isolates ex vivo (Figure 2C).

When phosphorylation of mTORC2 substrates was examined, the contrast was even more striking. OSI-027 markedly decreased phosphorylation of Akt at Ser⁴⁷³ in Jeko cells at 8 and 24 hours, whereas rapamycin had little or no effect (Figure 2D-E). Similar

results were observed in Jurkat cells, although higher OSI-027 concentrations were required to achieve the same degree of inhibition (Figure 2D). Consistent with these results, OSI-027 also inhibited phosphorylation of Akt at Ser⁴⁷³ in primary MCL isolates (Figure 2F).

Examination of Akt substrates revealed that phosphorylation of PRAS40 was inhibited by OSI-027 but not rapamycin (Figure 2D). Effects of OSI-027 on the phosphorylation of other Akt substrates were variable, with some (eg, Foxo3a, Figure 2E) showing limited dephosphorylation and others showing no effect at all (eg, GSK3 β , Figure 2E), in agreement with recent results showing heterogeneous effects of the dual mTORC1/mTORC2 inhibitor AZD8805 on Akt substrates.¹⁷

To determine the effect of OSI-027 on mTORC1 and mTORC2 assembly, the amounts of raptor and rictor bound to mTOR were examined in cells treated with OSI-027 for 24 hours. OSI-027 did not affect the total amount of raptor and rictor but did diminish the amount of rictor bound to mTOR, with less effect on the amount of raptor bound (Figure 2G).

Mechanism of inhibition of Akt phosphorylation by OSI-027

In addition to inhibiting mTORC2, there are several potential mechanisms by which OSI-027 could influence Akt phosphorylation at Ser⁴⁷³, including inactivation of signaling responsible for the priming phosphorylation of Akt on Thr³⁰⁸ or activation of Akt phosphatases. To rule out unsuspected inhibition of upstream signaling, we assessed Akt Thr³⁰⁸ phosphorylation. This modification, which is mediated by the PI3K/PDK1 pathway, was increased rather than decreased in these cells (Figures 3A-B). Likewise, PDK1 autophosphorylation at Ser²⁴¹ was not inhibited by OSI-027. Collectively, these results rule out the possibility that OSI-027 exerts its effects through unsuspected inhibition of PI3K, PDK1 or some other upstream signaling process.

In further experiments, we also examined the possibility that OSI-027 might affect Akt phosphatases. Immunoblotting demon-

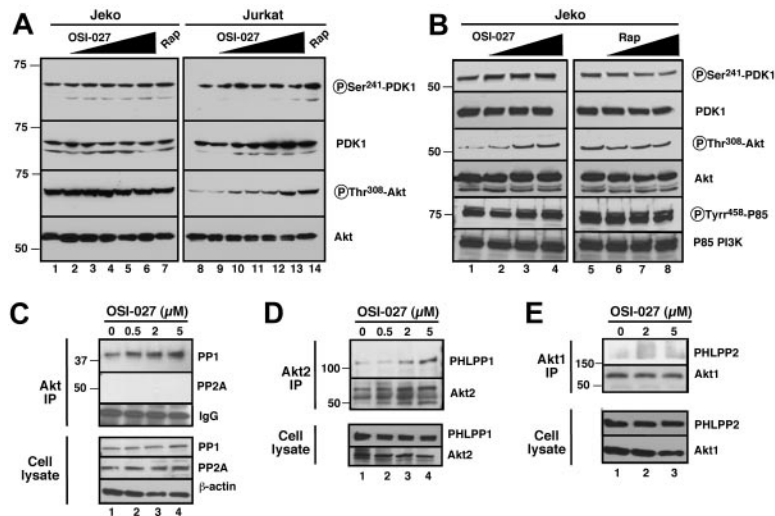


Figure 3. Effects of OSI-027 on Akt Thr³⁰⁸ phosphorylation and Akt-associated phosphatases. (A) Jeko (left) and Jurkat (right) cells were treated for 8 hours with diluent (lanes 1,8); OSI-127 at 1.25, 2.5, 5, 10 or 20 μ M (lanes 2-6 and 9-13, respectively); or 10nM rapamycin (lanes 7,14). Whole cell lysates²⁸ were then subjected to SDS-PAGE followed by immunoblotting with antibody that recognizes the indicated antigen. (B) Jeko cells were treated for 24 hours with diluent (lanes 1,5); OSI-127 at 0.5, 2, or 5 μ M (lanes 2-4); or rapamycin at 1, 10 and 100nM (lanes 6-8). Cell lysates²⁶ were then subjected to SDS-PAGE followed by immunoblotting with antibody that recognizes the indicated antigen. (C) After a 24-hour treatment with OSI-027, Akt immunoprecipitates (top) or cell lysates (bottom) from Jeko cells were probed with antibodies to PP1 and PP2A as indicated. (D, E) After a 24-hour treatment with OSI-027, immunoprecipitates of Akt2 (D) or Akt1 (E) from Jeko cells were probed for PHLPP isoforms as indicated. Additional experiments (not shown) indicated that PHLPP1 failed to immunoprecipitate with Akt1 and PHLPP2 failed to immunoprecipitate with Akt2.

strated that total cellular levels of protein phosphatase 1 (PP1), PP2, PH domain leucine-rich repeat protein phosphatase 1 (PHLPP1) and PHLPP2 were unaltered after a 24-hour exposure to OSI-027 (Figure 3C-E bottom panels). On the other hand, immunoprecipitation experiments suggested increased association of Akt isoforms with PP1 (Figure 3C top panel) as well as increased association of Akt2 with PHLPP1 (Figure 3D top panel), a phosphatase that has been specifically implicated in dephosphorylation at Akt2 Ser⁴⁷³.^{35,36} Thus, while inhibition of Akt phosphorylation at Ser⁴⁷³ undoubtedly reflects catalytic inhibition of mTORC2,¹⁹ we cannot rule out the possibility that increased dephosphorylation by Akt phosphatases also contributes.

Antiproliferative effect of OSI-027 in lymphoid cell lines

To assess the potential effects of dual mTORC1/mTORC2 inhibition, malignant lymphoid cell lines were treated with OSI-027, then examined using ³H-thymidine incorporation into DNA and MTS dye reduction assays. The thymidine incorporation assay revealed a dose-dependent inhibition of DNA synthesis in all 4 lines examined (Figure 4A), with 50% inhibition at concentrations ranging from < 0.5 μ M (Jeko and Mino) to 1 μ M (Jurkat) and > 95% inhibition at higher doses. In contrast, rapamycin was able to inhibit ³H-thymidine incorporation by only 50%-60% even at high concentrations in 3 of the 4 lines (Figure 4B).

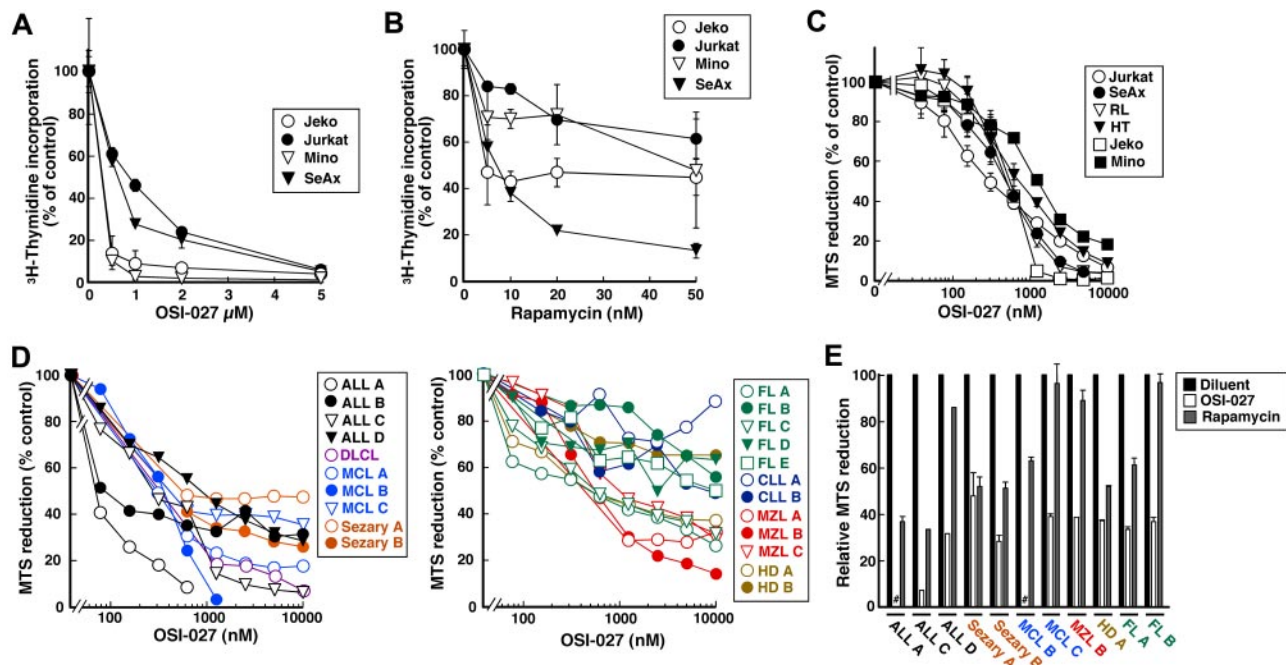


Figure 4. OSI-027 inhibits ³H-thymidine incorporation and diminishes viable cell mass in cultures of malignant lymphoid cells. (A-B) After lymphoid cell lines were treated for 48 hours with OSI-027 or rapamycin as indicated, ³H-thymidine incorporation into DNA was assayed. (C-E) After lymphoid cell lines (C) or primary clinical samples from patients with the indicated lymphoid neoplasms (D-E) were treated for 5 days with OSI-027 or rapamycin as indicated (C-D) or with 5 μ M OSI-027 versus 10nM rapamycin (E), MTS reduction was assayed. MTS reduction of cells treated with diluent (0.1% DMSO) for 5 days was set at 100% in each assay. Error bars in panels A through C, mean \pm SEM of 3 independent assays.

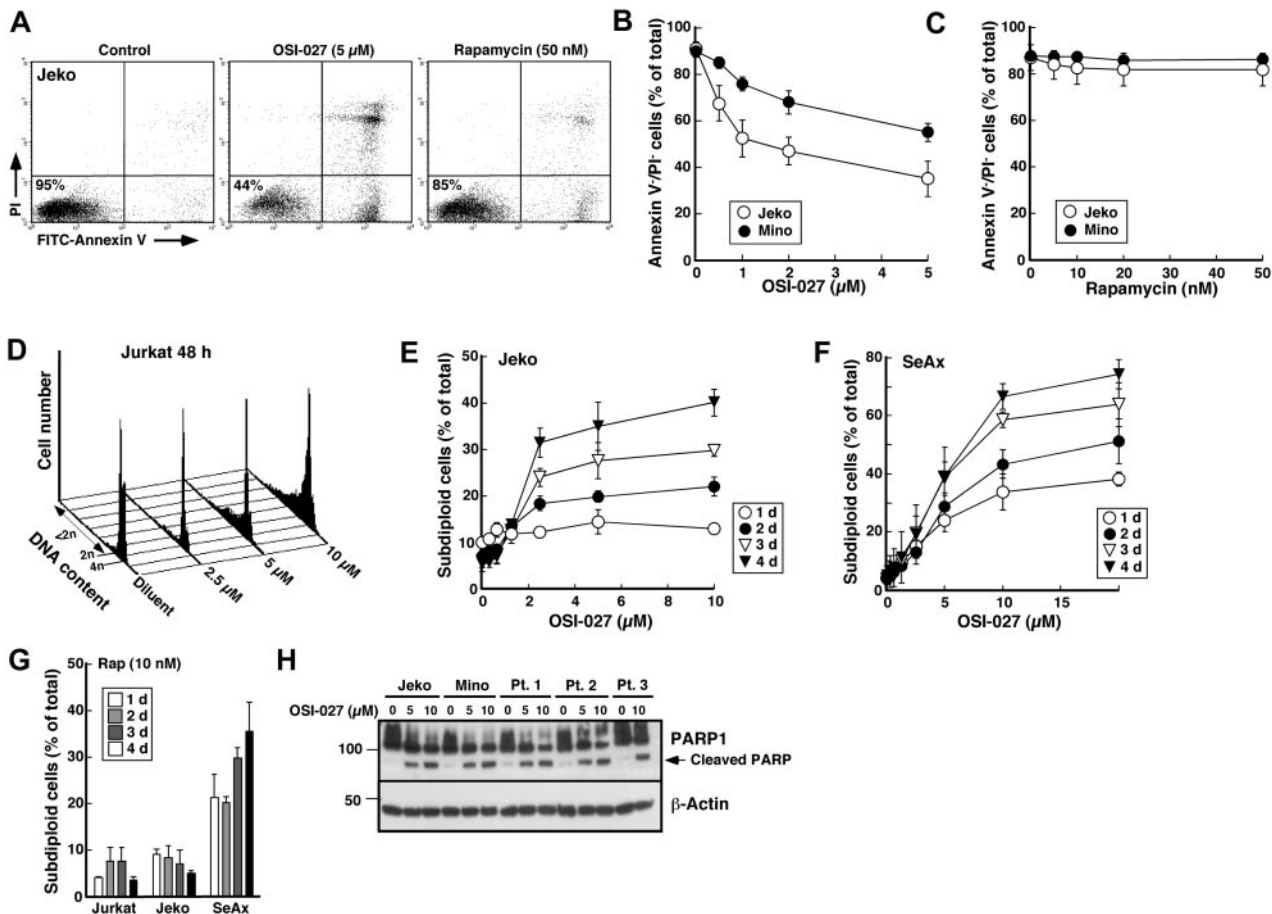


Figure 5. OSI-027 induces apoptosis in malignant lymphoid cell lines and clinical lymphoma samples. (A-C) Jeko and Mino cells were treated for 48 hours with the indicated concentrations of OSI-027 (B) and assayed using annexin V and PI as illustrated in panel A. Values in panels B and C represent the percentage of total cells that were negative for staining with annexin V and PI. (D) Jurkat were treated for 48 hours with the indicated concentrations of OSI-027, lysed in citric acid under conditions where fragmented DNA is extracted, stained with propidium iodide (PI) and subjected to flow microfluorimetry. Results of this and additional assays are summarized in Figure 6A. (E-G) Jeko, SeAx and Jurkat cells were treated for 24-96 hours with the indicated concentrations of OSI-027 (E-F) or 10nM rapamycin (G) and assayed as illustrated in panel D. (H) After treatment with diluent or OSI-027 for 48 hours, lysates from Jeko cells, Mino cells, or MCL samples from 3 separate patients were subjected to SDS-PAGE and probed with antibody to PARP1. Arrow, previously described caspase-induced PARP cleavage fragment.⁴⁸ Error bars in panels B, C, E, and F, mean \pm SEM of 3 independent assays.

To examine longer term effects of OSI-027, cells were treated with OSI-027 for 5 days and assayed for MTS reduction as an indication of viable cell mass. The lymphoid lines exhibited a range of sensitivities (Figure 4C), with IC₅₀ values ranging from 300nM (Jurkat) to 2 μ M (Mino). In comparison, all cell lines showed minimal sensitivity to rapamycin, with many not even showing a 50% reduction in viable cell mass (data not shown). Likewise, examination of clinical samples from patients with various lymphoid malignancies (supplemental Table 1, available on the *Blood* Web site; see the Supplemental Materials link at the top of the online article) revealed inhibition of MTS reduction after OSI-027 treatment (Figure 4D). Importantly, the IC₅₀ values ranged from 100nM in 2 ALL samples to 10 μ M in several follicular lymphomas, suggesting that some lymphoid neoplasms might be more sensitive than others. Direct comparison of the effects of 5 μ M OSI-027 and 10nM rapamycin revealed that OSI-027 exhibited greater effects in 10 of 11 clinical isolates encompassing several different lymphoid malignancies (Figure 4E).

OSI-027 induces cell death in malignant lymphoid cell lines

Because MTS assays do not distinguish between cell cycle arrest and cytotoxicity in continuously cycling cell lines, we next examined the mode of cell killing using various assays. Electron

microscopy revealed the presence of cells with classic features of apoptosis, including chromatin condensation and nuclear fragmentation, in Jurkat cells treated with OSI-027 (supplemental Figure 1). Flow cytometry demonstrated increased annexin V binding (Figure 5A) that occurred in a dose-dependent manner after treatment with OSI-027 (Figure 5B; see also Figure 6B) but not rapamycin (Figure 5C). Likewise, staining with propidium iodide followed by flow cytometry demonstrated that OSI-027 induced G₁ arrest (Figure 5D) and the appearance of subdiploid cells in a dose-dependent manner (Figure 5D-F; see also Figure 6A) in multiple cell lines, with the Sezary line SeAx being particularly sensitive (Figure 5F). Among the 8 lymphoid cell lines examined, only RL cells showed very limited induction of apoptosis after OSI-027 treatment (supplemental Figure 2A), possibly as a consequence of the high Bcl-2 expression that accompanies their t(8;14) chromosomal translocation (supplemental Figure 2C) and a Bcl-2 mutation that results in a particularly potent Bcl-2 sequence variant.²⁴ In the same experiments, rapamycin failed to induce apoptosis in all but the SeAx line (Figure 5C,G). In further studies, OSI-027-induced apoptosis was also detectable in cell lines and clinical MCL samples using caspase-mediated PARP cleavage as a readout (Figure 5H).

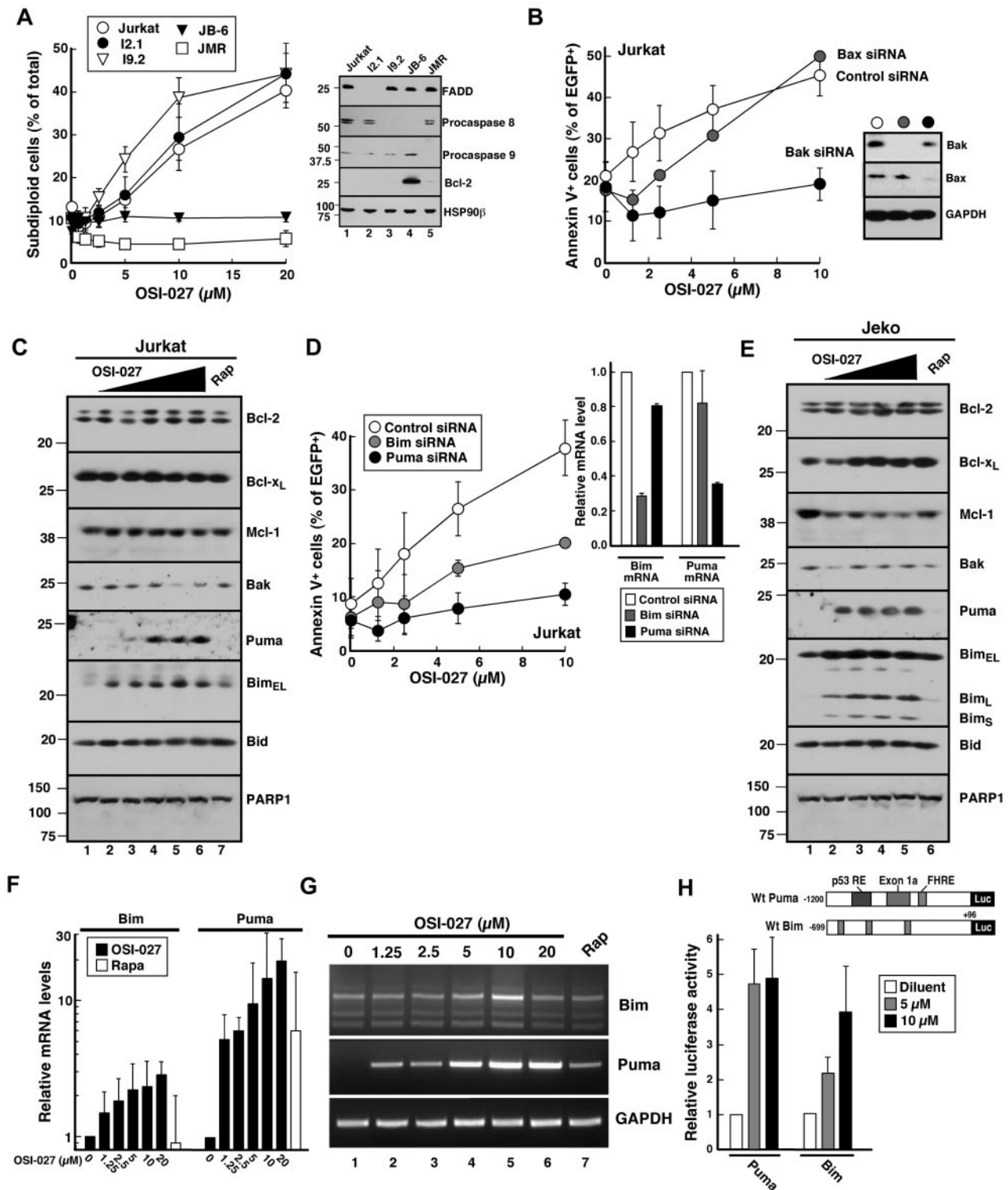


Figure 6. OSI-027 induces Puma- and Bim-dependent apoptosis. (A) Parental Jurkat cells and Jurkat variants lacking critical apoptotic pathway components (inset) were treated for 48 hours with OSI-027, stained with PI and analyzed as illustrated in Figure 5D. Error bars, mean \pm SEM of 3 independent assays. (B,D) Twenty-four hours after transfection with control siRNA or siRNA targeting Bax or Bak (B) or Bim or Puma (D) along with plasmid encoding EGFP-histone H2B (to mark successfully transfected cells), Jurkat cells were harvested to assess target down-regulation or treated for 48 hours with the indicated concentration of OSI-027, stained with APC-annexin V, and analyzed by 2-color flow cytometry to assess annexin V binding in EGFP-histone H2B⁺ cells. Error bars, mean \pm SEM of 3 independent assays. Insets, immunoblots (B) or qRT-PCR (D) demonstrating down-regulation of the targeted protein or message, respectively. (C,E) After Jurkat (C) and Jeko cells (E) were treated for 48 hours with diluent (lanes 1); OSI-027 at 1.25, 2.5, 5, 10 or 20 μM (lanes 2-6); or 10 nM rapamycin (lane 7) in the presence of the caspase inhibitor Q-VD-OPH (5 μM) to inhibit apoptosis,²² whole cell lysates²⁸ were subjected to SDS-PAGE followed by immunoblotting with antibodies that recognize the indicated antigen. PARP1 served as a loading control. (F-G) After Jurkat cells were treated for 48 hours with diluent, OSI-027 at the indicated concentration or 10 nM rapamycin in the presence of 5 μM Q-VD-OPH, RNA was isolated and subjected to conventional RT-PCR or qRT-PCR. Noxa and GAPDH served as controls. Results in panel F, geometric mean of 3 independent experiments. (H) Beginning 24 hours after transfection with the indicated reporter construct, Jurkat cells were treated for 48 hours with diluent or OSI-027 at the indicated concentration in the presence of 5 μM Q-VD-OPH and cell lysates were assayed for firefly luciferase. Error bars, mean \pm SD of 4-6 independent experiments.

In view of earlier reports that OSI-027, like rapamycin, can also induce autophagy,²¹ Jurkat cells were transfected with plasmid encoding LC3-EGFP, treated with OSI-027 or rapamycin, and examined by confocal microscopy for autophagosome formation. As indicated in supplemental Figure 3A-B, OSI-027 and rapamycin increased autophagy to the same extent. In further experiments, cells were treated with OSI-027 in the absence and presence of 3-methyladenine or chloroquine, 2 reported autophagy inhibitors.³⁷ As indicated in supplemental Figure 3C, 3-methyladenine enhanced OSI-027–induced killing slightly and chloroquine enhanced killing substantially, suggesting that the autophagy induced in lymphoid cells is protective rather than cytotoxic. Further experiments focused on the mechanism of OSI-027–induced cytotoxicity.

OSI-027 induces apoptosis through the mitochondrial pathway

Previous studies have shown that Akt regulates both the death receptor and mitochondrial apoptotic pathways (reviewed in Datta et al³⁸ and Duronio³⁹). In particular, Akt has been shown to catalyze an inhibitory phosphorylation of Foxo3a, which regulates expression of Fas and Fas ligand as well as several proapoptotic Bcl-2 family members. Accordingly, we used a series of Jurkat variants deficient in components of one pathway or the other to better define the process of OSI-027–induced apoptosis. Jurkat variants lacking caspase 8 (I9.2) or FADD (I2.1), 2 essential components of the death receptor pathway, were resistant to death ligands but were at least as sensitive as parental Jurkat cells to OSI-027 (Figure 6A). In contrast, Jurkat cells lacking caspase 9 (JMR) were resistant to OSI-027, as were Bcl-2 overexpressing JB-6 cells (Figure 6A). These results suggested that the mitochondrial pathway, but not the death receptor pathway, plays a critical role in OSI-027–induced apoptosis.

The mitochondrial pathway is regulated by Bcl-2 family members, which can be divided into at least 3 groups⁴⁰⁻⁴²: Bax and Bak, which participate in outer mitochondrial membrane permeabilization; BH3-only family members such as Bim and Puma, which are thought to directly activate Bax and Bak; and antiapoptotic family members such as Bcl-2, Bcl-x_L and Mcl-1, which prevent apoptosis by binding Bax, Bak and the BH3-only family members. Because activation of Bax or Bak is such an important event in apoptosis triggered through the mitochondrial pathway, parental Jurkat cells were treated with Bax or Bak siRNA before OSI-027 exposure. Down-regulation of Bax had relatively little impact on OSI-027–induced apoptosis (Figure 6B), consistent with the low Bax expression in this cell line.²⁷ In contrast, Bak down-regulation diminished apoptosis by at least 80% (Figure 6B), again confirming the importance of the mitochondrial pathway.

OSI-027 induced killing depends on Bim and Puma up-regulation

Because Bak activation results from changes in other pro- and antiapoptotic Bcl-2 family members,⁴⁰⁻⁴² further experiments examined changes in levels and activation of these polypeptides. Immunoblotting failed to demonstrate OSI-027–induced down-regulation of antiapoptotic Bcl-2 family members or up-regulation of Bax and Bak in Jurkat cells (Figure 6C and data not shown). In contrast, the BH3-only Bcl-2 family members Bim and Puma increased markedly during treatment with OSI-027 but not rapamycin (Figure 6C). Subsequent experiments demonstrated that siRNA-mediated down-regulation of Puma and, to a lesser extent, Bim protected cells from OSI-027–induced apoptosis (Figure 6D),

confirming the importance of these changes in OSI-027–induced killing. Similar up-regulation of Puma and Bim was observed in Jeko and SeAx cells as well (Figure 6E and supplemental Figure 4). Moreover, when cells were treated with the structurally distinct kinase inhibitor NVP-BEZ235 (supplemental Figure 5A), which in Jeko cells inhibits mTORC1 and mTORC2 at low concentrations (supplemental Figure 5B, phospho-Ser⁴⁷³-Akt, lanes 1-4) and PI3 kinase at higher concentrations (supplemental Figure 5B, phospho-Ser³⁰⁸-Akt, lanes 6 and 7), similar up-regulation of Puma and, to a lesser extent, Bim was observed beginning at concentrations that inhibit mTOR (supplemental Figure 5B lanes 1-4), suggesting that the up-regulation of these BH3-only proteins reflects a bona fide effect of inhibiting mTOR signaling. Semiquantitative and quantitative RT-PCR demonstrated increased mRNA encoding Puma and, to a smaller extent, Bim in multiple cell lines, including Jurkat, Jeko and SeAx after OSI-027 treatment (Figure 6F,G and supplemental Figure 4C). Moreover, luciferase reporter assays demonstrated OSI-027–induced activation of the PUMA and BIM promoters in Jurkat (Figure 6H) and SeAx cells (supplemental Figure 4D). Collectively, these results suggest that OSI-027 induces transactivation of the PUMA and BIM promoters, leading to up-regulation of these activator BH3-only proteins⁴³ and engagement of the mitochondrial apoptotic pathway.

Activity of OSI-027 in a lymphoma xenograft model

In further studies, we examined the effect of OSI-027 on the same events in vivo. Once Jeko xenografts were established, mice were treated daily for 6 days on/2 days off for 18 doses. On this schedule OSI-027 was well tolerated, with no animals requiring sacrifice for weight loss or other toxicities. Xenografts were harvested 4 hours after treatment on days 3, 5 and 6 to assess effects on apoptotic proteins or were followed for up to 35 days to assess xenograft growth.

Consistent with results observed in vitro, OSI-027 profoundly inhibited both mTORC1, as evidenced by diminished phosphorylation of 4EBP1 and S6, and mTORC2, as monitored by Akt Ser⁴⁷³ phosphorylation (Figure 7A). This was accompanied by a 4- to 6-fold increase in Puma message (Figure 7B) and increased Puma protein (Figure 7C) with little or no effect on Bim. Cleaved PARP was detectable in some xenografts by day 3 and in all xenografts by day 5 (Figure 7C), suggesting that apoptosis was occurring.

By day 12, when all animals receiving vehicle required sacrifice because of large lymphomatous masses, lesions on the flanks of OSI-027–treated animals were at or below baseline (Figure 7D-F). The Jeko xenografts not only stopped growing within 6 days of the initiation of OSI treatment (Figure 7D), but shrank to 39 ± 25% of pretreatment levels by the end of treatment (Figure 7F). When OSI-027 was discontinued, the residual lymphomatous masses began to regrow (Figure 7D). In a second experiment using the same exposure paradigm, OSI-027 at an even lower dose had a similar effect (Figure 7G). In contrast, doses of rapamycin that yield serum levels similar to those observed at the maximum tolerated dose in humans³² were strictly cytostatic (Figure 7G).

Discussion

Recent studies have shown that rapamycin and its analogues are active in a wide range of lymphoma subtypes.² The responses, however, are typically partial and short-lived. In the present study we have compared the dual mTORC1/mTORC2 inhibitor OSI-027

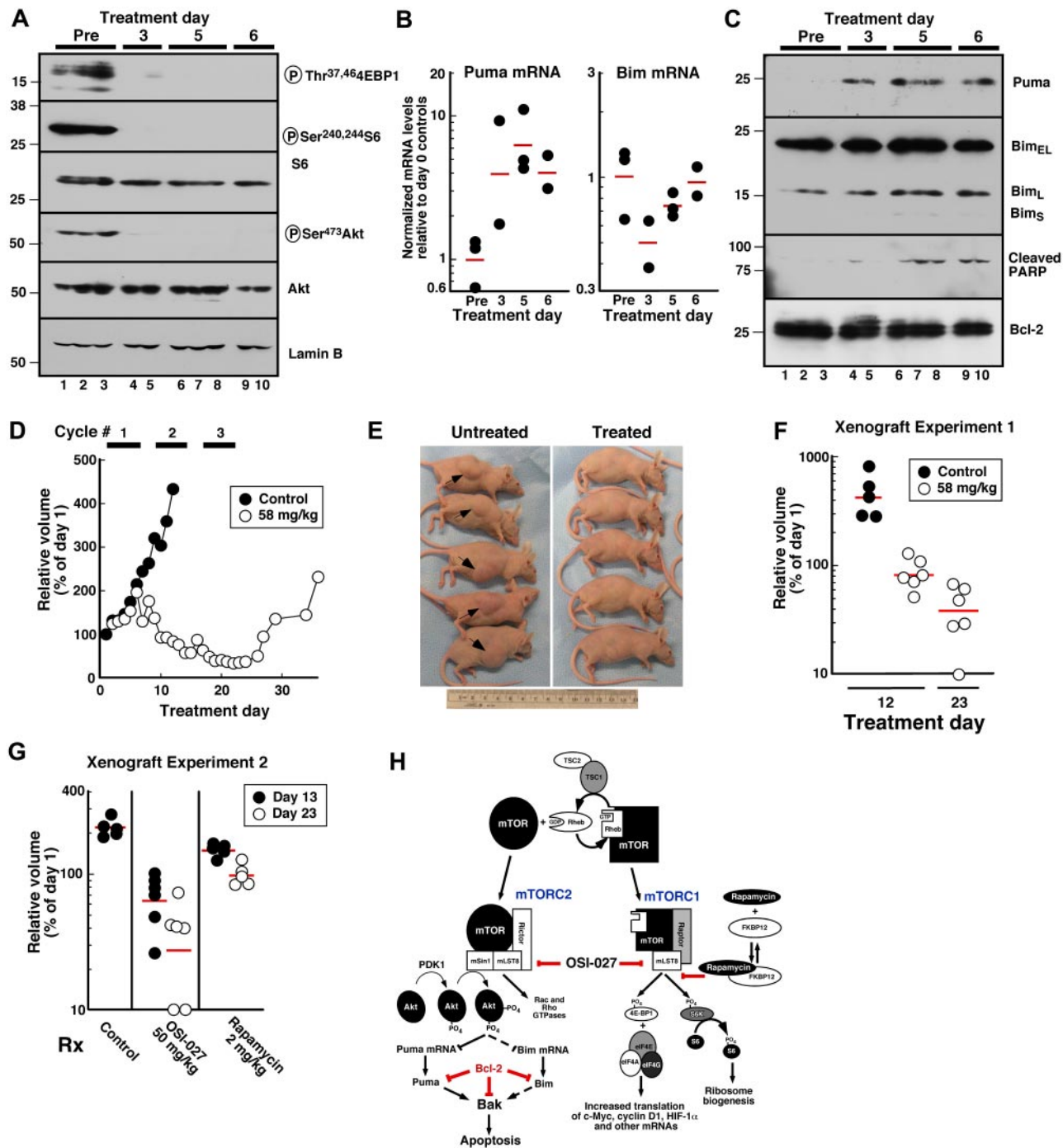


Figure 7. Activity of OSI-027 against Jeko xenografts in vivo. (A,C) Whole cell lysates prepared⁴⁹ from separate xenografts of untreated mice (lanes 1-3) or xenografts harvested 4 hours after treatment with OSI-027 on day 3 (lanes 4,5), day 5 (lanes 6-8) or day 6 (lanes 9,10) were subjected to SDS-PAGE and probed with antibodies to the indicated antigen. (B) qRT-PCR for Bim and Puma mRNA in xenografts harvested before treatment (Pre) or on days 3, 5 and 6 at 4 hours after OSI-027. Each symbol represents the mean of 3 values from 1 xenograft. Horizontal bars, geometric mean of samples from that day. (D) Mice bearing established xenografts were treated with 3 cycles of OSI-027 at 58 mg/kg orally on a 6 days on/2 days off schedule. Results shown are the geometric mean of 5 masses from control mice and 6 masses in 5 treated mice, with each value normalized to its pretreatment value. The mass that became undetectable was arbitrarily assigned a value of 10% of its pretreatment value. (E) Appearance of Jeko xenografts in diluent- and OSI-027-treated mice on day 12 when control animals needed to be killed because masses had reached institutional limits for size. (F) Relative volumes of each Jeko xenograft on day 12 when control animals were killed and on day 23 at the end of treatment. (G) Relative volumes of Jeko xenografts on day 13 (when control animals needed to be killed, closed circles) and day 23 (end of treatment, open circles) in a separate xenograft experiment in which animals were randomized to diluent, OSI-027 50 mg/kg or rapamycin 2 mg/kg on days 1-6, 9-14, and 17-22. Horizontal bars, geometric mean of 6 (OSI-027) or 5 (other groups) mice in treatment group. (H) Proposed mechanism of cytotoxicity of OSI-027 in lymphoid cells. Steps inhibited by rapamycin, OSI-027 and Bcl-2 are shown. Dashed lines indicate that up-regulation of Bim is more variable than Puma among different lymphoid cell lines.

to rapamycin in several preclinical models. Results of this analysis demonstrated that OSI-27 is more effective than rapamycin at inhibiting proliferation and inducing apoptosis in malignant lymphoid cells in vitro. Additional experiments not only established for the first time the mechanism of cytotoxicity of this class of agents

in human lymphoma cells as summarized in Figure 7H, but also demonstrated activity against lymphoma xenografts in vivo. Collectively, these results have important implications for future development of dual mTORC1/mTORC2 inhibitors as potential agents to treat lymphoid malignancies.

Our initial studies demonstrated that OSI-027 inhibits both mTORC1 and mTORC2 in lymphoid cells. Like rapamycin, OSI-027 inhibited phosphorylation of the mTORC1 substrate p70 S6 kinase and its downstream substrate S6. In contrast to rapamycin, however, which fails to inhibit phosphorylation of other mTORC1 substrates such as 4EBP1,¹¹ OSI-027 inhibited 4EBP1 phosphorylation on Thr³⁷ and Thr⁴⁶ (Figure 2A-B). Moreover, OSI-027 inhibited phosphorylation of Akt on Ser⁴⁷³, an mTORC2-mediated event (Figure 2D-E). This resulted in OSI-027–induced inhibition of the phosphorylation of several Akt substrates (eg, PRAS40 and Foxo3a), although phosphorylation of other substrates (eg, TSC2, GSK3 β and Foxo1) remained unchanged during the time course of the experiments (Figure 2 and data not shown). Importantly, in the model systems examined here, PDK1-mediated phosphorylation of Akt on Thr³⁰⁸ was not diminished by OSI-027 (Figure 3A-B), ruling out unsuspected inhibition of PI3K or PDK1 as a cause of diminished Akt activation. We are aware, however, that Akt Thr³⁰⁸ phosphorylation decreases after OSI-027 treatment in other cell lines, suggesting that this biochemical change might vary among different cell types.²⁰

Previous studies have demonstrated that dual mTORC1/mTORC2 inhibitors are active in preclinical models of Bcr/abl-driven leukemia, T-cell ALL and solid tumors.^{16-19,34,44} Although induction of apoptosis by these dual mTORC1/mTORC2 inhibitors has been described, the mechanism of cytotoxicity has been unclear. Earlier work demonstrated that rapamycin induces Mcl-1 down-regulation in some lymphoid cells,⁴⁵ possibly reflecting the short half-life of Mcl-1 when protein synthesis is inhibited. In accord with these results, we observed Mcl-1 down-regulation in some cell lines (Figure 6E), although this was much less evident in others (Figure 6C and supplemental Figure 4) even though OSI-027 induced apoptosis in both types of lines. Earlier reports also indicated that Akt, acting through FOXO transcription factors to control the expression of Fas ligand, can activate the death receptor pathway in certain cell types.³⁸ Our results using I9.2 and I2.1 cells, which lack caspase 8 and FADD, respectively, clearly show that cells lacking a functional death receptor pathway are still sensitive to OSI-027 (Figure 6A). In contrast, JMR cells, which lack caspase 9, are resistant to OSI-027 (Figure 6A), implicating the mitochondrial pathway in OSI-027–induced apoptosis.

The mitochondrial pathway is typically triggered by changes in the amount, activity, or localization of BH3-only Bcl-2 family members.⁴⁰⁻⁴² Among the BH3-only family members examined, Puma and (to a smaller and more variable extent) Bim increased at the mRNA and protein level after OSI-027 treatment (Figures 6,7 and supplemental Figure 4). Reporter assays demonstrated activation of the Puma and Bim promoters (Figure 6H, supplemental Figure 4C), suggesting OSI-027–induced activation of one or more transcription factors. Further studies, however, are required to determine whether additional changes also contribute to the up-regulation of these two BH3-only proteins. Puma mRNA appears to increase more than Puma promoter activity (Figure 6F-H), raising the possibility that mRNA stability has also been altered. Moreover, the effects of OSI-027 on Bim expression are more variable than Puma, possibly reflecting higher basal Bim expression before drug treatment or a difference in chromatin organization at the two promoters. Nonetheless, the present observations identify Puma up-regulation as a potential biomarker of mTOR inhibitor cytotoxicity that can be explored further in the future.

To the extent that Puma (and Bim) up-regulation contributes to OSI-027–induced cytotoxicity, one would predict that overexpression of antiapoptotic Bcl-2 family members might result in resistance even when mTORC1 and mTORC2 have been successfully inhibited (Figure 7H). Consistent with this prediction, we observed that JB-6 cells, a Jurkat variant expressing high levels of Bcl-2, were resistant to OSI-027–induced apoptosis (Figure 6A). Likewise, RL cells, which express high levels of a mutant, highly antiapoptotic Bcl-2 protein as a consequence of a t(14;18) translocation,^{24,27} were also resistant to OSI-027–induced apoptosis (supplemental Figure 2); and RL xenografts showed only growth suppression without any evidence of regression (data not shown). Thus, when all other factors are equal, it appears that Bcl-2 overexpression can be a mechanism of resistance to this class of agents, which might explain the lower sensitivity of follicular lymphoma and CLL specimens (Figure 4D right panel). On the other hand, when Bcl-2 is not so massively overexpressed or when the up-regulation of Bim and Puma is sufficient to neutralize Bcl-2, as in Jeko cells, robust induction of apoptosis *in vitro* and regression of xenografts *in vivo* is readily detectable (Figures 5 and 7). Moreover, because the cytotoxicity of OSI-027 depends on up-regulation of Puma and Bim, which can be neutralized by other antiapoptotic Bcl-2 family members, it is likely that the degree of up-regulation of Puma and Bim as well as the expression levels, affinities, and prior occupancy of several antiapoptotic Bcl-2 family members will factor into sensitivity or resistance when non-isogenic cell lines or clinical tumors are compared with each other.

In addition to its ability to induce apoptosis, OSI-027 also enhances autophagy (supplemental Figure 3).²¹ According to current understanding, the induction of autophagy involves recruitment of the BH3 protein Beclin-1 to a pre-autophagosome structure,⁴⁶ which would thereby free some of the cellular Bcl-2 and allow it to neutralize Puma and/or Bim. Consistent with such a model, our results (supplemental Figure 3C) and others²¹ suggest that autophagy protects cells from OSI-027–induced killing. In particular, results of the present study indicate that the autophagy inhibitor chloroquine is particularly effective at enhancing OSI-027–induced apoptosis (supplemental Figure 3C).

Our studies also indicate that the cytotoxic effects of OSI-027 take some time to develop. In Jurkat cells, for example, where a DNA damaging agent such as etoposide or a death ligand such as Fas ligand can induce apoptosis in as little as 2-4 hours,⁴⁷ it takes 48-72 hours of continuous OSI-027 exposure to induce apoptosis *in vitro* (eg, Figure 5D and 6A). Consistent with these results, we also observed a several day lag before induction of apoptosis in Jeko xenografts *in vivo* (Figure 7C). These observations, which likely reflect the time needed for Puma accumulation and Mcl-1 down-regulation, provide a potential explanation for the observation that established Jeko xenografts do not begin to regress until day 7 of treatment (Figure 7D).

The results observed Figure 7 not only provide the first evidence for potential efficacy of OSI-027 in lymphoid malignancies *in vivo*, but also suggest that the mechanism of cytotoxicity observed *in vitro* is also observed *in vivo*. In future studies it will be important to examine OSI-027 in additional models, including orthotopic xenografts or genetically engineered lymphoma models in which lymphoma cells encounter more physiologic survival signals.

In addition to its activity against established cell lines, OSI-027 diminished cell survival as measured by diminished MTS reduction in clinical samples of lymphoid malignancies

(Figure 4D-E). Because cells in these samples were not proliferating appreciably in vitro, these results likely reflect induction of apoptosis, as confirmed in a smaller number of samples by immunoblotting for cleaved PARP (Figure 5H). While these effects of OSI-027 were observed in samples representing several lymphoid malignancies, including MCL, marginal zone lymphoma, Sezary syndrome, and ALL (Figure 4D), follicular lymphoma and CLL specimens were notably less sensitive, possibly reflecting the role of Bcl-2 up-regulation in the pathogenesis of these disorders.

In summary, the present results provide the first demonstration of antiproliferative and proapoptotic activity of a dual mTORC1/mTORC2 inhibitor in established lymphoid cell lines and primary specimens from several lymphoid malignancies. These studies establish the critical role of Puma up-regulation in the mechanism of cytotoxicity of this class of drugs as well as at least one potential mechanism of resistance. This class of agents appears to warrant further preclinical and possible clinical testing in wide range of lymphoid malignancies.

Acknowledgments

Kind gifts of reagents and cell lines from G. Widley, P. Howe, W. Wu, A. T. Look, and I. Schmitz are gratefully acknowledged.

References

- Jemal A, Siegel R, Xu J, Ward E. Cancer statistics, 2010. *CA Cancer J Clin*. 2010;60(5):277-300.
- Witzig TE, Gupta M. Signal transduction inhibitor therapy for lymphoma. *Hematology Am Soc Hematol Educ Program*. 2010;2010:265-270.
- Bjornst MA, Houghton PJ. The TOR pathway: a target for cancer therapy. *Nat Rev Cancer*. 2004;4(5):335-348.
- Dowling RJ, Topisirovic I, Fonseca BD, Sonenberg N. Dissecting the role of mTOR: lessons from mTOR inhibitors. *Biochim Biophys Acta*. 2010;1804(3):433-439.
- Sengupta S, Peterson TR, Sabatini DM. Regulation of the mTOR complex 1 pathway by nutrients, growth factors, and stress. *Mol Cell*. 2010;40(2):310-322.
- Guertin DA, Sabatini DM. Defining the role of mTOR in cancer. *Cancer Cell*. 2007;12(1):9-22.
- Ma XM, Blenis J. Molecular mechanisms of mTOR-mediated translational control. *Nat Rev Mol Cell Biol*. 2009;10(5):307-318.
- Easton JB, Houghton PJ. mTOR and cancer therapy. *Oncogene*. 2006;25(48):6436-6446.
- Chiang GG, Abraham RT. Targeting the mTOR signaling network in cancer. *Trends Mol Med*. 2007;13(10):433-442.
- Edinger AL, Linardic CM, Chiang GG, Thompson CB, Abraham RT. Differential effects of rapamycin on mammalian target of rapamycin signaling functions in mammalian cells. *Cancer Res*. 2003;63(23):8451-8460.
- Choo AY, Yoon SO, Kim SG, Roux PP, Blenis J. Rapamycin differentially inhibits S6Ks and 4E-BP1 to mediate cell-type-specific repression of mRNA translation. *Proc Natl Acad Sci U S A*. 2008;105(45):17414-17419.
- Sabatini DM. mTOR and cancer: insights into a complex relationship. *Nat Rev Cancer*. 2006;6(9):729-734.
- Hsu PP, Kang SA, Rameseder J, et al. The mTOR-regulated phosphoproteome reveals a mechanism of mTORC1-mediated inhibition of growth factor signaling. *Science*. 2011;332(6035):1317-1322.
- Zeng Z, Sarbassov dos D, Samudio IJ, et al. Rapamycin derivatives reduce mTORC2 signaling and inhibit AKT activation in AML. *Blood*. 2007;109(8):3509-3512.
- Abraham RT, Gibbons JJ. The mammalian target of rapamycin signaling pathway: twists and turns in the road to cancer therapy. *Clin Cancer Res*. 2007;13(11):3109-3114.
- Yu K, Shi C, Toral-Barza L, et al. Beyond rapalog therapy: preclinical pharmacology and antitumor activity of WYE-125132, an ATP-competitive and specific inhibitor of mTORC1 and mTORC2. *Cancer Res*. 2010;70(2):621-631.
- Chresta CM, Davies BR, Hickson I, et al. AZD8055 is a potent, selective, and orally bioavailable ATP-competitive mammalian target of rapamycin kinase inhibitor with in vitro and in vivo antitumor activity. *Cancer Res*. 2010;70(1):288-298.
- Janes MR, Limon JJ, So L, et al. Effective and selective targeting of leukemia cells using a TORC1/2 kinase inhibitor. *Nat Med*. 2010;16(2):205-213.
- Falcon BL, Barr S, Gokhale PC, et al. Reduced VEGF production, angiogenesis, and vascular regrowth contribute to the antitumor properties of dual mTORC1/mTORC2 inhibitors. *Cancer Res*. 2011;71(5):1573-1583.
- Bhagwat SV, Gokhale PC, Crew AP, et al. Preclinical characterization of OSI-027, a potent and selective inhibitor of mTORC1 and mTORC2: distinct from rapamycin. *Mol Cancer Ther*. 2011;10(8):1394-1406.
- Carayol N, Vakana E, Sassano A, et al. Critical roles for mTORC2- and rapamycin-insensitive mTORC1-complexes in growth and survival of BCR-ABL-expressing leukemic cells. *Proc Natl Acad Sci U S A*. 2010;107(28):12469-12474.
- Caserta TM, Smith AN, Gultice AD, Reedy MA, Brown TL. Q-VD-OPH, a broad spectrum caspase inhibitor with potent antiapoptotic properties. *Apoptosis*. 2003;8(4):345-352.
- Meng X, Chandra J, Loegering D, et al. Central role of FADD in apoptosis induction by the mitogen activated protein kinase kinase inhibitor CI1040 (PD184352) in acute lymphocytic leukemia cell lines in vitro. *J Biol Chem*. 2003;278(47):47326-47339.
- Smith AJ, Dai H, Correia C, Lee S-H, Takahashi R, Kaufmann SH. Noxa/Bcl-2 interactions contribute to bortezomib resistance in human lymphoid cells. *J Biol Chem*. 2011;286(20):17682-17692.
- Mesa RA, Loegering D, Powell HL, et al. Heat shock protein 90 inhibition sensitizes acute myelogenous leukemia cells to cytarabine. *Blood*. 2005;106(1):318-327.
- Gupta M, Ansell SM, Novak AJ, Kumar S, Kaufmann SH, Witzig TE. Inhibition of histone deacetylase overcomes rapamycin-mediated resistance in diffuse large B-cell lymphoma by inhibiting Akt signaling through mTORC2. *Blood*. 2009;114(14):2926-2935.
- Dai H, Meng XW, Lee S-H, Schneider PA, Kaufmann SH. Context-dependent Bcl-2/Bak Interactions Regulate Lymphoid Cell Apoptosis. *J Biol Chem*. 2009;284(27):18311-18322.
- Kaufmann SH, Svingen PA, Gore SD, Armstrong DK, Cheng Y-C, Rowinsky EK. Altered formation of topotecan-stabilized topoisomerase I-DNA adducts in human leukemia cells. *Blood*. 1997;89(6):2098-2104.
- Kaufmann SH. Reutilization of immunoblots after chemiluminescent detection. *Anal Biochem*. 2001;296(2):283-286.
- Wildev GM, Howe PH. Runx1 is a co-activator with FOXO3 to mediate transforming growth factor beta (TGFbeta)-induced Bim transcription in hepatic cells. *J Biol Chem*. 2009;284(30):20227-20239.
- Wu WS, Heinrichs S, Xu D, et al. Slug antagonizes p53-mediated apoptosis of hematopoietic progenitors by repressing puma. *Cell*. 2005;123(4):641-653.
- Phung TL, Ziv K, Dabydeen D, et al. Pathological

The authors also thank H. Dai and A. Smith for numerous helpful suggestions.

This work was supported in part by National Institutes of Health grants R01 CA127433 (T.E.W.) and R01 CA069008 (S.H.K.), a Career Development Award from the University of Iowa/Mayo Clinic SPORE P50 CA97274 (M.G.), a gift from the General Mills Foundation to the Mayo Foundation Clinician Investigator Training Program (A.E.W.H.), and the Henry J. Predolin Foundation.

Authorship

Contribution: M.G., A.E.W.H., and S.H.K. designed research, performed research, analyzed data and wrote paper. S.S.Y., J.J.H., P.A.S., B.D.K., M.S., L.W., J.C.S., K.L.P., and K.S.F. performed research. A.D.H., B.D.S. and J.E.K. provided new reagents. S.B. provided new reagents and wrote paper. T.E.W. designed research and wrote paper.

Conflict-of-interest disclosure: S.B. is an employee of OSI Pharmaceuticals. The remaining authors declare no competing financial interests.

Correspondence: Scott Kaufmann, MD, PhD, Mayo Clinic, Gonda 19, 200 First St, SW, Rochester, MN 55905; e-mail: kaufmann.scott@mayo.edu; or Thomas E. Witzig, MD, Mayo Clinic, Stable 6-28, 200 First St, SW, Rochester, MN 55905; e-mail: witzig@mayo.edu.

- angiogenesis is induced by sustained Akt signaling and inhibited by rapamycin. *Cancer Cell*. 2006;10(2):159-170.
33. Gupta M, Dillon SR, Ziesmer SC, et al. A proliferation-inducing ligand mediates follicular lymphoma B-cell proliferation and cyclin D1 expression through phosphatidylinositol 3-kinase-regulated mammalian target of rapamycin activation. *Blood*. 2009;113(21):5206-5216.
 34. Evangelisti C, Ricci F, Tazzari P, et al. Targeted inhibition of mTORC1 and mTORC2 by active-site mTOR inhibitors has cytotoxic effects in T-cell acute lymphoblastic leukemia. *Leukemia*. 2011;25(5):781-791.
 35. Gao T, Fumari F, Newton AC. PHLPP: a phosphatase that directly dephosphorylates Akt, promotes apoptosis, and suppresses tumor growth. *Mol Cell*. 2005;18(1):13-24.
 36. Brognard J, Sieracki E, Gao T, Newton AC. PHLPP and a second isoform, PHLPP2, differentially attenuate the amplitude of Akt signaling by regulating distinct Akt isoforms. *Mol Cell*. 2007;25(6):917-931.
 37. Amaravadi RK, Lippincott-Schwartz J, Yin XM, et al. Principles and current strategies for targeting autophagy for cancer treatment. *Clin Cancer Res*. 2011;17(4):654-666.
 38. Datta SR, Brunet A, Greenberg ME. Cellular survival: a play in three Akts. *Genes Dev*. 1999;13:2905-2927.
 39. Duronio V. The life of a cell: apoptosis regulation by the PI3K/PKB pathway. *Biochem J*. 2008;415(3):333-344.
 40. Taylor RC, Cullen SP, Martin SJ. Apoptosis: controlled demolition at the cellular level. *Nat Rev Mol Cell Biol*. 2008;9(3):231-241.
 41. Youle RJ, Strasser A. The BCL-2 protein family: opposing activities that mediate cell death. *Nat Rev Mol Cell Biol*. 2008;9(1):47-59.
 42. Chipuk JE, Moldoveanu T, Llambi F, Parsons MJ, Green DR. The BCL-2 family reunion. *Mol Cell*. 2010;37(3):299-310.
 43. Ren D, Tu HC, Kim H, et al. BID, BIM, and PUMA are essential for activation of the BAX- and BAK-dependent cell death program. *Science*. 2010;330(6009):1390-1393.
 44. Yu K, Toral-Barza L, Shi C, et al. Biochemical, cellular, and in vivo activity of novel ATP-competitive and selective inhibitors of the mammalian target of rapamycin. *Cancer Res*. 2009;69(15):6232-6240.
 45. Wei G, Twomey D, Lamb J, et al. Gene expression-based chemical genomics identifies rapamycin as a modulator of MCL1 and glucocorticoid resistance. *Cancer Cell*. 2006;10(4):331-342.
 46. Kang R, Zeh HJ, Lotze MT, Tang D. The Beclin 1 network regulates autophagy and apoptosis. *Cell Death Differ*. 2011;18(4):571-580.
 47. Meng XW, Heldebrandt MP, Kaufmann SH. Phorbol-12-myristate 13-acetate inhibits death receptor-mediated apoptosis in Jurkat cells by disrupting FADD recruitment. *J Biol Chem*. 2002;277(5):3776-3783.
 48. Lazebnik YA, Kaufmann SH, Desnoyers S, Poirier GG, Earnshaw WC. Cleavage of poly-(ADP-ribose)polymerase by a proteinase with properties like ICE. *Nature*. 1994;371(6495):346-347.
 49. Friedman HS, Dolan ME, Kaufmann SH, et al. Elevated DNA polymerase alpha, DNA polymerase beta, and DNA topoisomerase II in a melphalan-resistant rhabdomyosarcoma xenograft that is cross-resistant to nitrosoureas and topotecan. *Cancer Res*. 1994;54(13):3487-3493.